Waste Management 88 (2019) 347–355

Contents lists available at ScienceDirect

Waste Management

journal homepage: www.elsevier.com/locate/wasman

Renewable aromatics through catalytic flash pyrolysis of pineapple crown leaves using HZSM-5 synthesized with RHA and diatomite

Andrey S. Barbosa [a], Lorena A.M. Siqueira [a], Rodolfo L.B.A. Medeiros [a,b], Dulce M.A. Melo [a,b,c], Marcus A.F. Melo [b,d], Julio C.O. Freitas [c], Renata M. Braga [a,e,*]

[a] Universidade Federal do Rio Grande do Norte, Laboratório de Tecnologia Ambiental, Natal, RN 59078-970, Brazil
[b] Universidade Federal do Rio Grande do Norte, PPGCEM, Natal, RN 59078-970, Brazil
[c] Universidade Federal do Rio Grande do Norte, Instituto de Química, Natal, RN 59078-970, Brazil
[d] Universidade Federal do Rio Grande do Norte, Dep. Engenharia Química, Natal, RN 59078-970, Brazil
[e] Universidade Federal do Rio Grande do Norte, Escola agrícola de Jundiaí – EAJ, Macaíba, RN 59280-000, Brazil

ARTICLE INFO

Article history:
Received 11 October 2018
Revised 24 March 2019
Accepted 24 March 2019
Available online 30 March 2019

Keywords:
Catalytic pyrolysis
Deoxygenation
HZSM-5
Rice husk ash
Pineapple crown leaves
Renewable aromatic compounds

ABSTRACT

The influence of reactor temperature of 300 and 600 °C and the acidity of the ZSM-5 and HZSM-5 catalysts on the pyrolysis product yields of the pineapple crown leaves have been investigated in a fixed bed reactor Py-GC/MS. The ZSM-5 catalyst was hydrothermally synthesized with a Si/Al ratio 50, using residual diatomite and rice husk ash as alternative sources of Al and Si for catalyst cost reduction. For the HZSM-5 synthesis, calcined ZSM-5 was activated by ion exchange between Na^+ and H^+. The catalysts structure was confirmed by the XRD and Rietveld treatment, SEM, FTIR, FRX, TGA and BET results. Analytical pyrolysis of the biomass was carried out at 500 °C in a Py-5200 HP-R pyrolyzer connected to the GC/MS and the pyrolysis vapors were transported to a catalytic bed at 300 and 600 °C. The results showed that the increase in the catalytic bed temperature promoted increased the aromatic content. The main pyrolysis products of the PCL were oxygenated compounds that were converted at 600 °C using the HZSM-5 catalyst into high value renewable aromatic compounds for the chemical industry, such as benzene, toluene, xylene, etilbenzene, thereby confirming the deoxygenation activity of synthesized catalyst to produce renewable aromatics compounds which are important platform chemicals and precursors for jet fuels, gases, polymers and solvents.

1. Introduction

Renewable aromatics compounds are important building blocks that can partially replace petrochemical resources in producing biofuel and chemicals. They can reduce dependence on oil and avoid environment impacts, due to less SO_x and CO_2 emission, increasing sustainable economies (Yang et al., 2017; Mei et al., 2018). Compounds such as phenols, benzene and toluene (among other monoaromatics) can be obtained by different biomass conversion routes into products. The thermochemical process such as pyrolysis, hydrothermal upgrading and gasification followed by the Fischer-Tropsch have been described to convert biomass into fuel (Gutiérrez-Antonio et al., 2017).

The pyrolysis of lignocellulosic materials and especially lignin-rich biomass, such as kraft lignin, eucalyptus and lignin containing crop, has been reported as a suitable process to produce phenol and other oxygenated aromatic compounds (Kurnia et al., 2017; Mei et al., 2018; Santana et al., 2018). However, the presence of several oxygenated compounds in bio-oil is responsible for lowering their calorific value, increasing corrosiveness, viscosity and chemical instability, thus decreasing its quality for biorefinery (French and Czernik, 2010; Lorenzetti et al., 2016; Mei et al., 2018). Some upgrading methods such as the use of zeolites can be applied in the pyrolysis process for deoxygenation of bio-oil to improve its quality for application as biofuel or as source of chemicals.

Catalytic pyrolysis has been identified as one of the most promising processes to selectively obtain specific chemicals and/or bio-oil with better physical and chemical properties (Stefanidis et al., 2011). Different materials have been evaluated for use as catalysts and special attention has been given to ZSM-5 due to its ability to produce aromatic compounds (Mihalcik et al., 2011; Kubička and Kikhtyanin, 2015). Alternative sources of Si and Al such as magadiite, kaolin, rectorite (Cui et al., 2018;

* Corresponding author at: Escola Agrícola de Jundiaí, RN 160, Km 03, Distrito de Jundiaí, Macaíba, RN 59280-000, Brazil.
E-mail address: renatabraga.r@gmail.com (R.M. Braga).

https://doi.org/10.1016/j.wasman.2019.03.052
0956-053X/

Holmes et al., 2011; Yue et al., 2014) were used in the synthesis of low-cost zeolites. However, many of these minerals are pretreated by use expensive reagents. Studies involving alternative and low-cost catalytic materials such as modified zeolites, clays and inorganic wastes are still limited. High silica residues, such as fly ash, rice husk ash and low-cost aluminosilicates, are promising materials for the synthesis of zeolites, as they present Si and Al that are fundamental to the zeolitic structure. The challenge is to match adequate biomass compositional with selectively efficient catalysts to produce renewable industrial products of interest.

Several biomass sources can be used in fast pyrolysis processes but special attention has been given to lignocellulosic waste, such as pinewood and eucalyptus sawdust, cotton stalk, corn stover and also industrial kraft lignins, with high energetic density and abundance in order to minimize the environmental impacts caused by their disposal (Efika et al., 2018; Karmee, 2018; Raviv et al., 2018; Shah et al., 2019). A recent study shows that pineapples crown leaves presents high energetic potential for application in thermochemical processes (Braga et al., 2015). Pineapple crowns represent 25% wt. of the fruit, being considered waste since it is discarded during consumption. Reusing and applying this biomass to the catalytic fast pyrolysis process is promising due to its abundance worldwide, its lignin content and energetic requirements for pyrolysis such as high volatiles content (78.84%), high bulk density (420.8 kg/m^3), low ash (5.22%) and fixed carbon content (6.98%) (Braga et al., 2015).

Therefore, the aim of this study was to evaluate the efficiency of ZSM-5 and HZSM-5 zeolite catalysts synthesized with low cost Si and Al alternative sources, in deoxygenation of pineapple crown leaves (PCL) pyrolysis products, which is an agricultural waste that will be used as a renewable source of hydrocarbons.

2. Materials and methods

2.1. Pineapple crown leaves (PCL) biomass

Pineapple crown leaves (PCL) were collected in the State of Paraíba, Brazil, and are a lignocellulosic agricultural waste which present high heating value 18.9 MJ/kg and apparent density (420.8 kg/m^3), in addition to important characteristics for application in the pyrolysis process such as low ash (5.2%) and moisture content (8.9%), and high volatile content (78.8%) (Fig. 1). The study described by Braga et al. (2015) confirms the energy potential available per unit mass of this biomass for the pyrolysis process.

The PCL was dried in an oven at 100 °C for 16 h and ground in a Willey macro-slicer, with selected particle size between 0.074 and 0.104 mm (Fig. 1) for application in the Py-GC/MS process.

2.2. Catalysts synthesis

The ZSM-5 was hydrothermally synthesized using tetrapropylammonium bromide (TPABr) as template, sodium hydroxide (NaOH) and powder diatomite residue, containing 88.53% SiO_2, 10.02% Al_2O_3, 0.48% TiO_2, 0.42% Fe_2O_3 and 0.35% K_2O, as source of Si and Al. The Si/Al ratio of zeolite was corrected to 50 with the addition of rice husk ash (RHA) containing 96% SiO_2, 2.18% K_2O, 0.86% P_2O_5 and 0.49% CaO. The diatomite was dispersed in NaOH solution and then a TPABr solution was added, followed by stirring and addition of RHA. The mixture was placed in a 250 mL becker and kept under stirring at 40 °C for 1 h. The synthesis followed the molar ratio of 10.6 TPABr: 14.3 Na_2O: 2.0 Al_2O_3: 100 SiO_2: 2000 H_2O. The catalysts were calcined in a tubular furnace at 550 °C, 5 °C min^{-1} for 4 h under a flow of 100 mL min^{-1} of N_2 during the first 2 h of isotherm, followed by calcination in an oxidizing atmosphere under a flow of 100 mL min^{-1} to the end of the process in order to minimize structural damage in the zeolite, given that large amounts of vapors are released by the zeolite pores during direct heating of the template. For HZSM-5 synthesis, the calcined ZSM-5 was activated by ion exchange between Na^+ and H^+. Initially 5 g of the zeolite was transferred to a flat bottom flask and 250 mL of NH_4Cl 1 M was added. The mixture was kept under stirring at 80 °C and reflux for 2 h. Then the formed suspension was vacuum filtered and washed with distilled water to remove the Cl^- and NH_4^+ ions which did not exchange. The process was repeated 3 times to effectively guarantee the ion exchange. The solid obtained was oven dried at 100 °C and calcined to activate the HZSM-5 zeolite acid site, where NH_3 is released by burning and the H^+ proton activates its acid sites. Calcination was carried out under the same conditions as described above.

2.3. Catalysts characterization

The catalysts calcination temperature was determined by thermogravimetric analysis (TGA), performed in a TA Instruments SDT Q600 balance, from room temperature to 900 °C, at 10 °C min^{-1}, under 100 mL min^{-1} of N_2, using approximately 10 mg of the sample. The zeolite crystalline phases were identified by X-ray diffraction using Shimadzu XRD-7000 with Cu-K α radiation source (λ = 1.5409 Å), voltage of 30 kV, current of 30 mA, step of 0.02° and speed of 0.01°/s. The data were collected in the range of 2θ from 0.5 to 10°. Rietveld refining was performed to confirm the zeolite structure and to obtain the network parameters. The morphology of the zeolite was identified by a Shimadzu SSX 550 SuperScan scanning electron microscope, equipped with the tungsten filament operating at 15 kV. The samples were previously

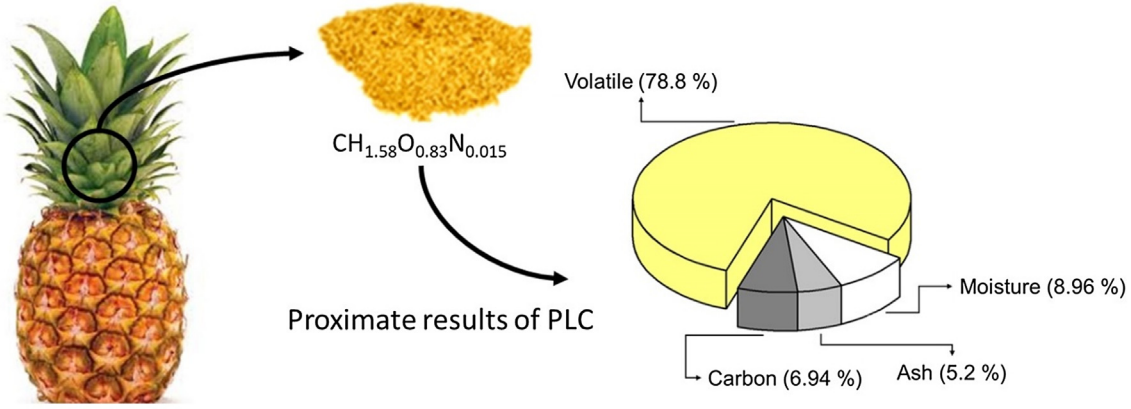

Fig. 1. Empirical molecular formula and proximate results of pineapple crown leaves (PLC).

covered with a thin layer of gold of approximately 70 nm to guarantee the electrical conductivity necessary for the analysis. Infrared absorption spectra were obtained from 4000 to 400 cm^{-1} using the Prestige-21 IR spectrophotometer from Shimadzu. The specific area and pore diameter of the calcined catalysts were calculated by the BET and BJH methods, respectively. The samples were degassed at 200 °C for 2 h and then analyzed in a Nova 2000 from Quanta Chrome Instruments.

2.4. Catalytic flash pyrolysis (Py-GC/MS)

The PCL pyrolysis was performed in a CDS Analytical Pyroprobe 5200 HP-R at 500 °C with a heating rate of 10.0 °C ms^{-1}, using approximately 1 mg of biomass, placed between the top and bottom quartz wool in a quartz tube (25.38 mm × 1.75 mm ID). The pyrolysis vapors were carried 50 mL min^{-1} of N_2 (99.999%) to a Tenax trap for desorption at 300 °C, transferred through a transfer line heated at 300 °C and injected at split mode of 1:50 in a GC-MS/MS 3900 VARIAN. The products were separated by a ZB-5MS column (60 m × 0.25 mm × 0.25 μm) using He as the carrier gas (1 mL min^{-1}). The column oven temperature program was as follows: at a constant temperature of 40 °C for 4 min, 40–280 °C at 10 °C min^{-1}, 280 °C constant for 14.5 min. The vapors produced in catalytic pyrolysis were previously directed to a catalytic bed heated at 300 and 600 °C with approximately 20 mg of the catalyst, before being at Tenax trap and then injected into the GC/MS 3900 VARIAN in the same conditions as conventional pyrolysis. MS detection was carried out under electron ionization (EI) of 70 eV and *m*/*z* range of 40–500. Peak identification was done by searching the NIST mass spectra library, considered identified at a similarity above 85%. Semi-quantitative analysis was performed based on the ratio of peak area and biomass mass used in the pyrolysis (Area/mg of biomass).

3. Results and discussion

3.1. Catalysts characterization

The thermogravimetric analysis (TGA) results of the non-calcined ZSM-5 (Fig. 2) showed three mass loss events. Moisture desorption is observed in the first one, while organic template (TPABr) degradation occurs in the second between 230 and 480 °C, and finally amine coke degradation from the template residues occurs in the last one above 480 °C (Zhang et al., 2017). The temperature of 550 °C was chosen for material calcination from the TGA results.

Fig. 3 shows the X-ray patterns of the synthesized materials. The ZSM-5 and HZSM-5 structures were confirmed by the pattern (01-079-1638 and 01-080-0922 JCPDS files, respectively), where the diffraction lines located at 2θ = 7.8, 8.7, 23.11, 23.90, 23.90 and 24.4° positions are characteristic of the zeolite structure. The crystalline structure of the orthorhombic type with Pnma space group was confirmed by the Rietveld method, where the lattice parameters presented in Table 1 are similar to those of the conventional zeolites. Only a small increase in the unit cell dimensions was observed for the zeolite submitted to ion exchange treatment (HZSM-5), and no secondary phase was identified. This result confirms the efficiency of the synthesis using low cost alternative Si and Al sources, maintaining the zeolite structural characteristics.

The FTIR spectra of Fig. 4 showed the vibrations, stretches and deformations of symmetrical and asymmetric siloxane groups, both internal and external to the zeolite structure. The bands at 3470 cm^{-1} of weak intensity represent the deformation of the T—O—H (Si or Al) group and O—H deformation of water on the surface of the zeolites (Sabarish and Unnikrishnan, 2017). Calcination may result in the disappearance of the absorption bands attributed to the template, thus the ZSM-5 (NC) zeolite spectrum shows weak C—H stretch absorption bands in the 2985–2880 cm^{-1} region due to the organic structure of the TPABr, after the calcination the bands are no longer verified (Ali, 2003). The band at 1640 cm^{-1} has been attributed to deformations in the water molecule absorbed on the surface of zeolite during the synthesis or during sample preparation with KBr (Narayanan et al., 2016). After the ion exchange treatment with aqueous ammonium chloride solution, a 1470 cm^{-1} band appears due to the N—H stretching and deformation modes, reminiscent of the NH_4^+ ions. The 1225 cm^{-1} band corresponds to the asymmetric stretch of the T—O—T group of the tetrahedron TO_4 (Ali, 2003; Xue et al., 2012). Bands 799 and 1089 cm^{-1} are respectively assigned to the symmetrical and asymmetric stretching of the T—O—T bond. The 451 cm^{-1} band

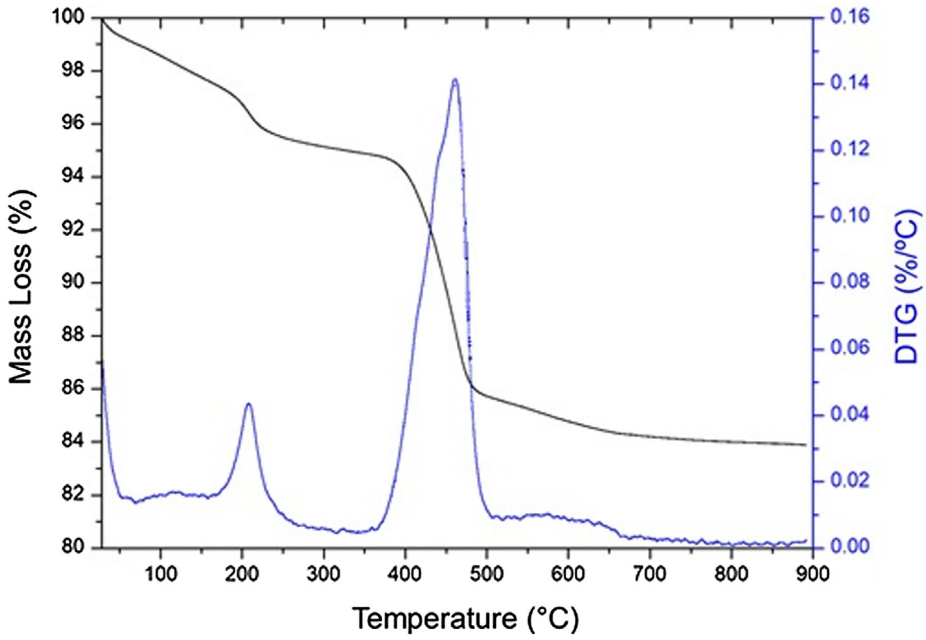

Fig. 2. ATG/DTG thermogravimetric analysis of non-calcined ZSM-5.

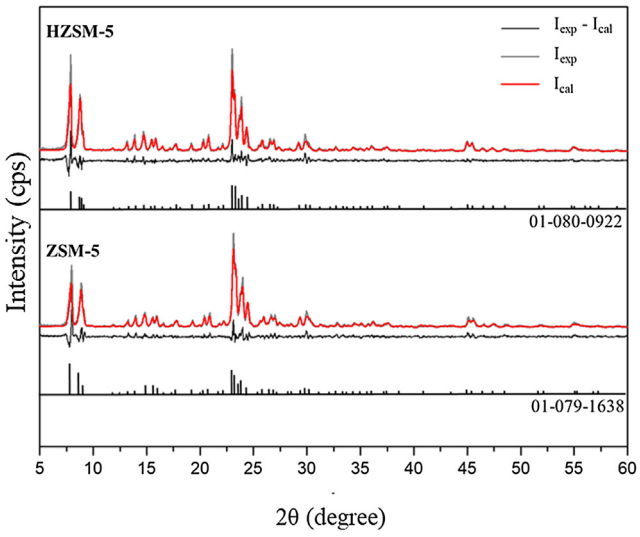

Fig. 3. XRD patterns of ZSM-5 and HZSM-5.

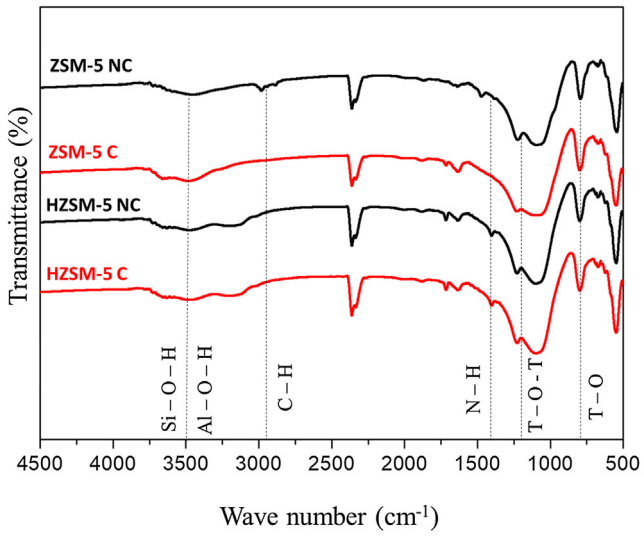

Fig. 4. FTIR spectra of calcined (C) and non-calcined (NC) ZSM-5 and HZSM-5.

Table 1
Rietveld refinement data for the catalysts.

Rietveld refinament data	Catalysts	
	ZSM-5	HZSM-5
Space group	Pnma	Pnma
λ (Å), Cukα	1.5409	1.5409
Data collection temperature T (°C)	25	25
a (Å)[a]	20.0605	20.1447
b (Å)[a]	19.8193	19.9357
c (Å)[a]	13.3404	13.4110
V (Å^3)[b]	5303.9	5385.8
GoF[c]	1.97	1.88
Rw (%)	18.35	17.12
CIF used[d]	66,648	68,734

[a] Cell lattice.
[b] Cell volume.
[c] Goodness of fit.
[d] Crystallograph information file.

represents the vibrations of the TO bond deformation of the internal SiO_4 and AlO_4 tetrahedral and the 545 cm^{-1} vibrations correspond to the asymmetric stretching of the double-membered (D5R) rings of the ZSM-5 zeolite's pentassyl structure (Ali, 2003; Yue et al., 2015).

Predominantly cubic morphology with some spherical particles were observed in the SEM results (Fig. 5), with mean particle size of less than 2 μm, similar to zeolites synthesized by the traditional route. The HZSM-5 showed a small reduction of the average particle size after the ion exchange treatment. The specific area for both ZSM-5 and HZSM-5 zeolites was 340.5 and 357.2 m^2/g, and 40.5 and 40.1 Å pore diameter, respectively. In this case, the ion exchange treatment did not promote significant changes in the texture properties of the zeolites.

3.2. Catalytic flash pyrolysis (Py-GC/MS)

The PLC pyrolysis presented different classes of oxygenated compounds as products, such as phenols, alcohols, ketones, and carboxylic acids (among others), as shown in Fig. 6 and Table 2. The composition and distribution of pyrolysis products are associated with the elemental composition and compositional characteristics of the biomass. Therefore, the predominance of oxygenated products is related to the high oxygen content, being 49% O, 44% C, 6% H and 0.9% N, which compose cellulose macromolecules (12.9%), hemicellulose (35.5%) and lignin (26.4%) biomass (Braga et al., 2015). The PLC presented high levels of hemicellulose and lignin, respectively, when compared with other biomasses applied in the pyrolysis process, such as 24.4 and 28% softwood (Demirbas, 1997), 27 and 19% sugar cane bagasse (Al Arni et al., 2010), 24 and 23.4% elephant grass (Braga et al., 2014) and 31.4 and 12% swicth grass, respectively (Reshamwala et al., 1995). These molecules are broken after the thermal degradation, forming compounds of smaller molecular masses and with greater thermal stability. The high phenolic compounds content identified among pyrolysis products is associated with lignin decomposition, and furan-type compounds are generally related to hemicellulose decomposition and part of the cellulose (Demirbaş, 2000; Yang et al., 2007; Wang et al., 2014; Wu et al., 2016). Thus, the high concentration of compounds such as 2,5-dimethylfuran, 2(5H)-Furanone, 3-Furaldehyde, 3-Furanmethanol, 2,4-dimethylfuran is associated with the high hemicellulose content of PCL. Phenolic compounds such as 2-methylphenol and 4-methylphenol are formed from the demethoxylation reactions of guaiacyl groups, such as 2-methoxy-4-vinylphenol present in the structure of the lignin molecule. The formation of compounds such as 4-methoxyphenol and 2,6-methoxyphenol possibly occurs due to the cracking of syringyl groups of the lignin macromolecule (Mohan et al., 2006; Carrier et al., 2011).

Light C_1—C_4 compounds have been identified as acetic acid, anhydride acetic and methyl acetate, and are derived from the thermal cracking reactions of larger molecular weight compounds, such as levoglycosan which is primarily formed by the thermal cleavage of β-1,4-glycosidic of cellulose (Wu et al., 2016).

The catalytic pyrolysis of PLC using ZSM-5 and HZSM-5 with alternative Si and Al sources significantly reduced the volatiles content, as can be observed by reducing the sum of peak areas of the chromatograms in Fig. 7, in addition to the reduction in oxygenated compounds. The increase in the temperature of the catalytic bed promoted the increase of the aromatic concentration and decrease of the C_1—C_4 compounds, suggesting secondary reactions in which these light compounds react on the surface of the catalyst to form aromatics, as proposed in the literature (Mohan et al., 2006). In general, the increase in reaction temperature promotes the decomposition of biomass into small molecules, as reported in the literature (Wang et al., 2015; Wang et al., 2014; Jia et al., 2017; Cheng and Huber, 2011). The increase in catalytic

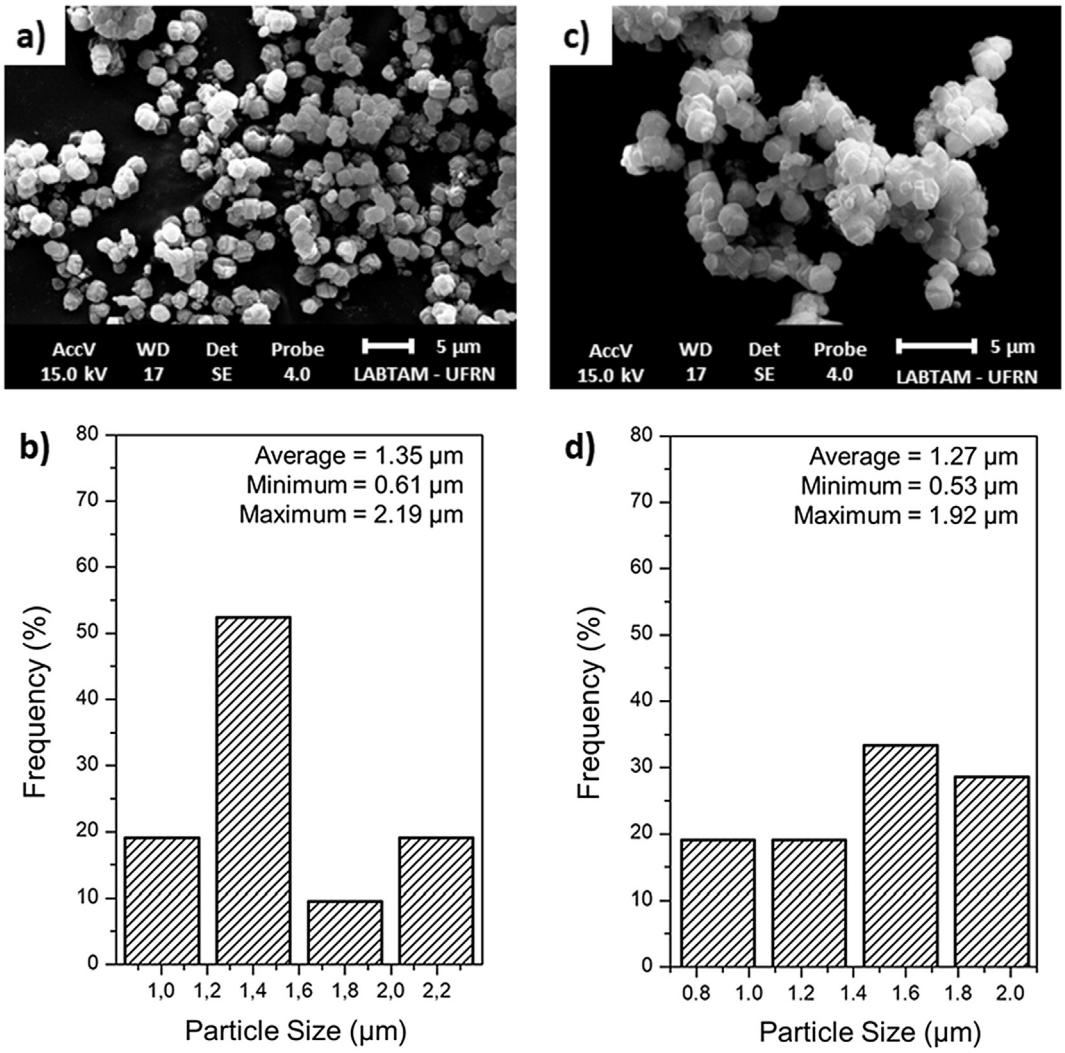

Fig. 5. SEM images and particle distribution of the ZSM-5 (a and b) and HZSM-5 (c and d).

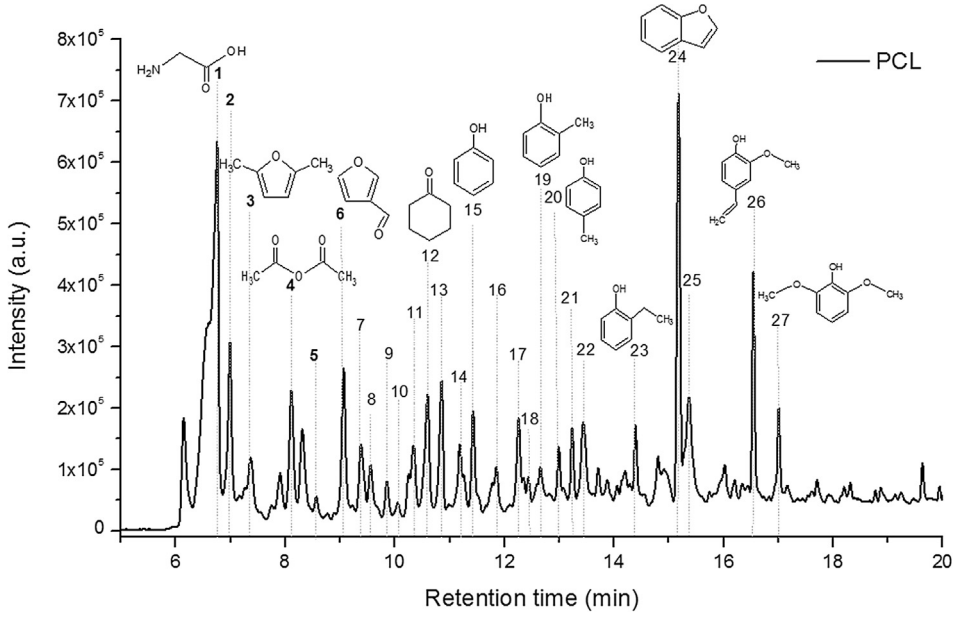

Fig. 6. Chromatogram of conventional pyrolysis products of PCL.

Table 2
Description of retention time, compounds, and peak areas of the pyrolysis products of PCL.

Peak	RT[a] (min)	Compound (WM)	*m/z*	CAS No.	PCL Area/mg (10^5)
1	6.7	C_1—C_4	–	64-19-7	59.2–64.2
2	7.0	Glicine ($C_2H_5NO_2$)	75	54-40-6	9.6–10.7
3	7.3	2,5-dimetilfurano (C_6H_8O)	96	625-86-5	2.6-2.7
4	8.1	Acetic anhydride ($C_4H_6O_3$)	102	108-24-7	6.7–8.8
5	8.5	2(5H)-furanone ($C_4H_8N_2$)	84	497-23-4	0.8–1.0
6	9.0	Furfural ($C_5H_4O_2$)	96	498-60-2	8.8–12.1
7	9.3	3-furanmethanol ($C_5H_6O_2$)	98	98-00-0	4.4–6.0
8	9.5	Diacetamide ($C_4H_7NO_2$)	101	6102-98-3	2.1–2.4
9	9.8	2H-pyran-2-one ($C_5H_4O_2$)	96	504-31-4	1.8–2.3
10	10.0	Estirene (C_8H_8)	104	100-42-5	0.7–0.8
11	10.3	2,4-dimethyl-furan (C_6H_8O)	96	3710-43-8	6.1–7.4
12	10.6	Cycloexanone ($C_6H_{10}O$)	98	108-94-1	7.1–7.7
13	10.8	2-cyclohexen-1-one (C_6H_8O)	96	930-68-7	7.5–7.6
14	11.2	5-methyl-2-furancarbaldehyde (C_6H_6O2)	110	620-02-0	2.1–2.5
15	11.4	Phenol (C_6H_6O)	94	108-95-1	4.4–4.6
16	11.8	*N*-buthyl-*tert*-buthylamine ($C_8H_{19}N$)	129	16486-74-1	1.0–1.0
17	12.2	3-methyl-1,2-cyclopentanedione ($C_6H_8O_2$)	112	765-70-8	3.7–3.7
18	12.4	2,3-dimethyl-2-cyclopenten-1-one ($C_7H_{10}O$)	110	1121-05-7	0.7–0.7
19	12.6	2-methylphenol (C_7H_8O)	108	95-48-7	1.1–1.0
20	13.0	4-methylphenol (C_7H_8O)	108	106-44-5	1.8–2.0
21	13.2	4- metoxyphenol ($C_7H_8O_2$)	124	150-76-5	3.0–3.1
22	13.4	3-buten-2-ol (C_4H_8O)	72	598-32-3	5.0–6.4
23	14.4	2-ethyl-phenol ($C_8H_{10}O$)	122	90-00-6	2.6–2.9
24	15.2	2,3-dihydro-benzofuran (C_8H_8O)	120	496-12-2	19.2–19.8
25	15.4	5-(hydroxymethyl)-2-furancarboxaldehyde ($C_6H_6O_3$)	126	67-47-0	4.0–5.5
26	16.6	2-metoxy-4-vinylphenol ($C_9H_{10}O$)	150	7786-61-0	8.5–8.8
27	17.0	2,6-metoxyphenol ($C_8H_{10}O_3$)	154	2033-89-8	3.1–3.3

[a] Retention time.

bed temperature to 600 °C favored the cracking of C—O bonds, justifying the generation of aromatic compounds such as benzene and toluene as shown in Fig. 8. These results are in agreement with the literature as reported by Onwudili et al. (2018) whose evaluated the influence of FCC reaction temperature (500 and 600 °C) using commercial zeolites Y and ZSM-5, in which they observed the same phenomena. However, this work brings as a differential the influence of the treatment on the surface and the comparison with a lower temperature (300 °C) that better clarifies the effects, since not only the acid form of the zeolite influences the selectivity to toluene and benzene as well as the reaction temperature.

Conventional PCL pyrolysis generated a total of 75×10^5 (Area/mg) of furan-like compounds which were converted to aromatics over HZSM-5. Recent studies have shown that furan compounds from pyrolysis of lignocellulosic biomasses can be catalytically converted to aromatic compounds using commercial HZSM-5 (45–60 Si/Al) acid zeolites (Carlson et al., 2009; Mullen and Boateng, 2010; Lorenzetti et al., 2016), thus confirming the conversion of the high content of furans into aromatics over synthesized HZSM-5 in the present work. Maneffa et al. (2016) demonstrated the formation of aromatics through fast catalytic pyrolysis of lignocellulosic biomass by three stages: (i) first the formation of anhydrous sugars from the cellulose or hemicellulose macromolecules; (ii) these sugars are then dehydrated to form furans; (iii) which then undergo various types of reactions on the acid zeolite, and finally are converted into aromatic compounds. Mullen and Boateng (2010) demonstrated that the primary oxygenated products of pyrolysis react on HZSM-5 type catalysts forming olefins that generate monoaromatic compounds. Both mechanisms can act on the catalytic pyrolysis of PCL over HZSM-5, as this catalyst has acidic sites that can directly deoxygenate of furan, ketones and other compounds via the route shown in Fig. 9.

Demethoxylation reactions of guaiacyl and syringyl groups present in the structure of the lignin molecule can directly form xylan compounds and oleofins which can be converted into benzene, as proposed in Fig. 9. Sustainable aromatics such as p-xylene are currently produced by Anellotech, Inc. from the conversion of various types of lignocellulosic biomass (wood residues, corn straw, sugarcane bagasse) into aromatics through rapid catalytic pyrolysis (Maneffa et al., 2016).

The best results for the catalytic pyrolysis of PCL were obtained using HZSM-5 with a catalytic bed temperature of 600 °C, which favored forming aromatic compounds. Kim et al. (2015) analyzed the Si/Al (30–280) parameter of commercial HZSM-5 in the pyrolysis of lignin extracted from poplar wood, verifying that acidity is inversely proportional to Si/Al ratio, and this factor is also responsible by increasing the yield of the aromatic content and by choosing a Si/Al ratio (50) with excellent acidity for the HZSM-5 catalyst synthesized in this work. The increase in aromatic content is reported in the literature as a function of the amount and strength of acid sites present in the catalysts (Mihalcik et al., 2011; Stefanidis et al., 2011; Engtrakul et al., 2016). Both the acidity and the catalytic bed temperature were responsible for increasing the aromatic content, since the highest yield of these compounds was evidenced at 600 °C for both catalysts, being even greater for the catalyst in its acid form (HZSM-5). The channel and pore sizes of ZSM-5 and HZSM-5 were enlarged when the reaction occurred at 600 °C, thereby increasing the conversion of oxygenates to aromatics (Yu et al., 2012; Kurnia et al., 2017). On the other hand, in the catalytic pyrolysis carried out at 300 °C few compounds were observed in the chromatograms. In this case, according to Cheng and Huber (2011) the aromatic and olefin is preferably produced at temperatures above 400 °C, because at low temperatures the pyrolysis vapors can be polymerized and condensed into the internal structure of HZSM-5. This is an important factor to explain the low aromatics production for PCL reactions with ZSM-5 and HZSM-5 at 300 °C.

Furan-type compounds were also observed in the pyrolysis products of biomass using ZSM-5, which confirms the importance of acid sites for deoxygenation reactions. Compounds of high

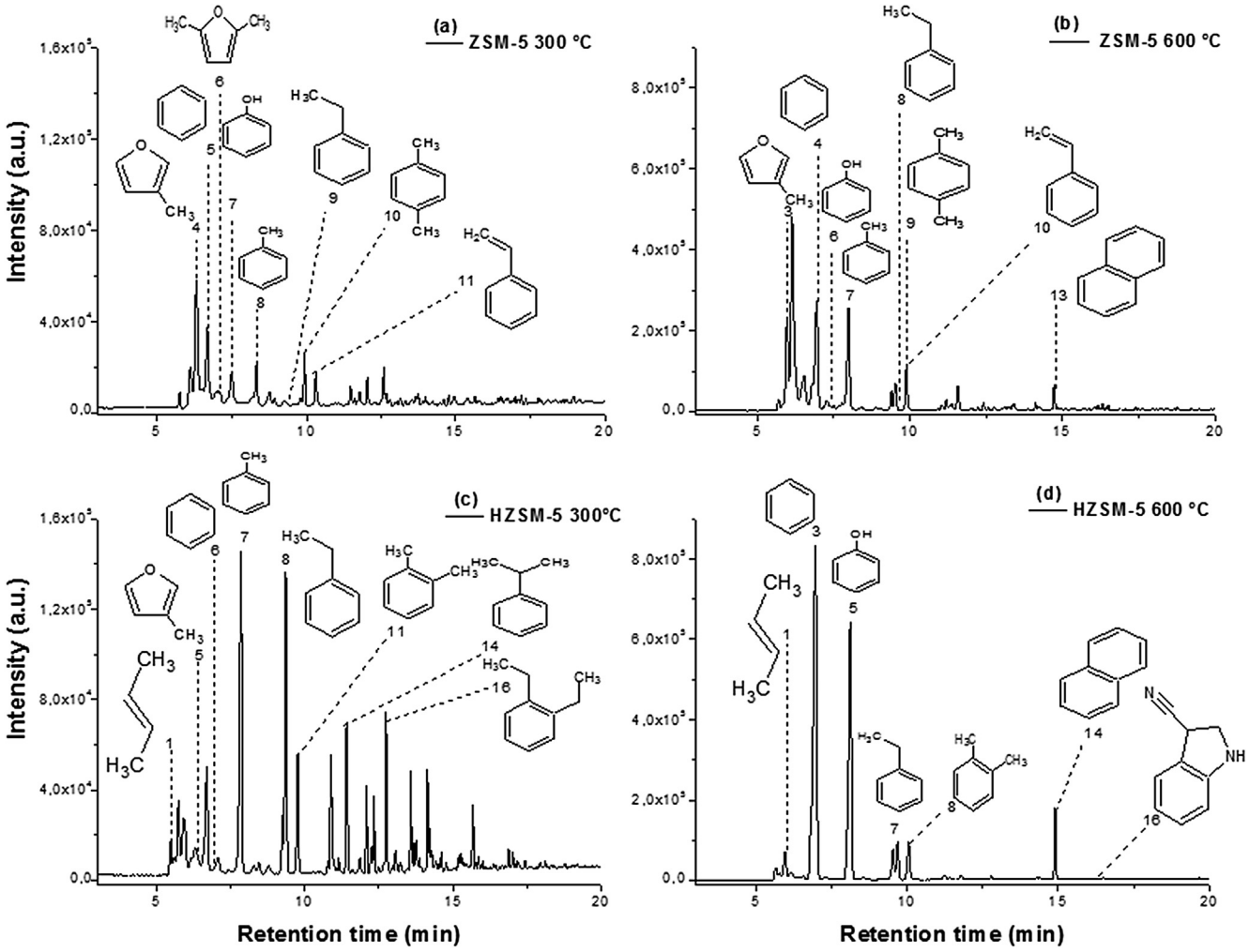

Fig. 7. Chromatograms of catalytic pyrolysis products of (a) ZSM-5 at 300 °C, (b) ZSM-5 at 600 °C, (c) HZSM-5 at 300 °C and (d) HZSM-5 at 600 °C.

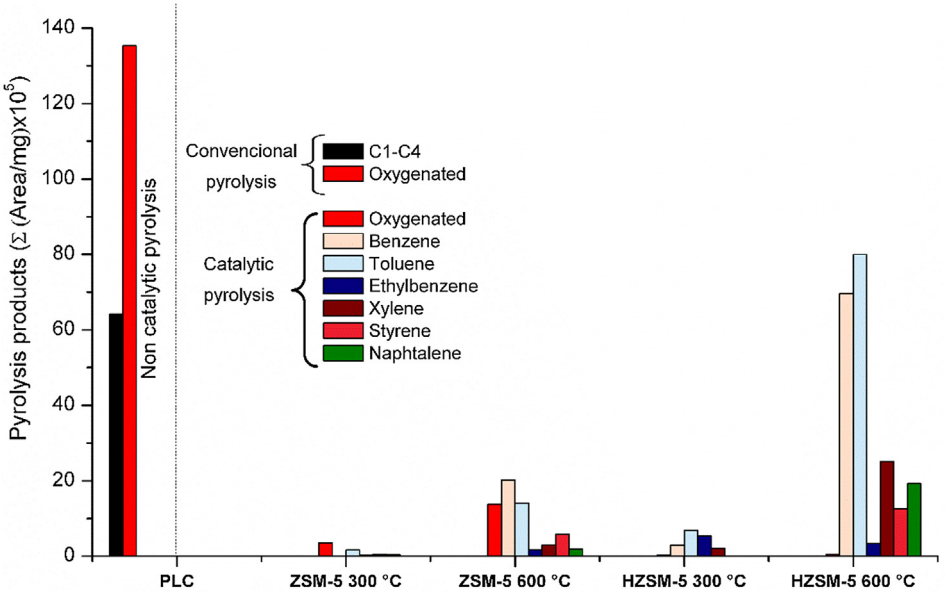

Fig. 8. Product distribution in non-catalytic and catalytic pyrolysis using ZSM-5 and HZSM-5.

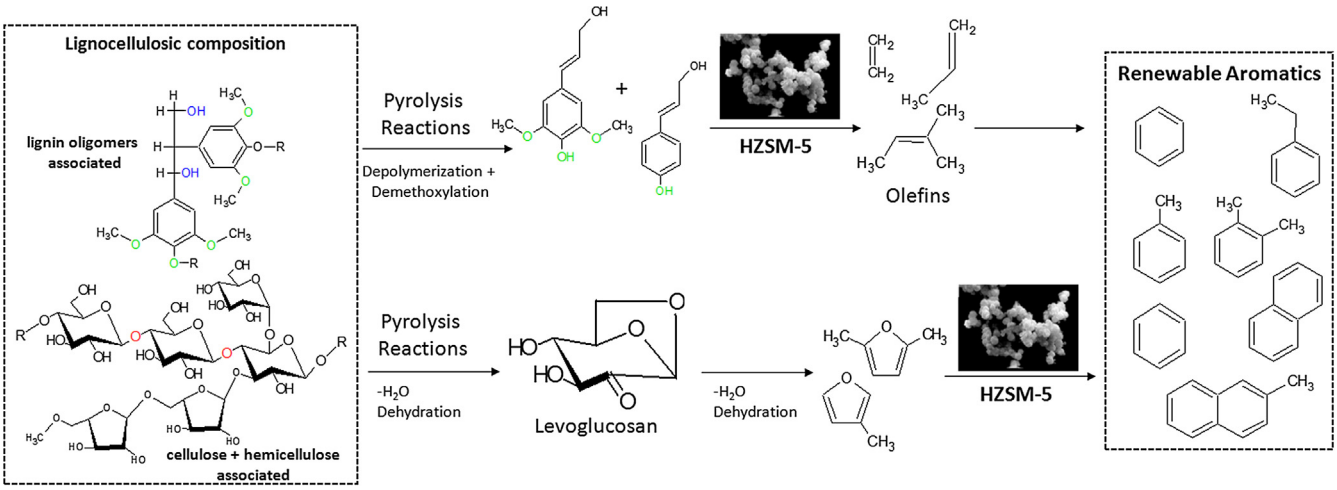

Fig. 9. Proposed pathway for formation of aromatics over HZSM-5.

industrial value were indentified among the aromatic compounds present in the PCL pyrolysis using HZSM-5 (Fig. 8) such as toluene, benzene, xylene, naphthalene, styrene and ethylbenzene.

4. Conclusion

In this study the catalytic activity of HZSM-5 synthesized with low cost Si and Al sources was demonstrated for producing aromatic compounds via flash pyrolysis of the agricultural waste from pineapple production (PCL). Most of the products formed in these reactions are aromatic compounds of industrial interest such as benzene, toluene, ethylbenzene and xylene. The monoaromatic production confirms the deoxygenation performance of catalyst which can act in the same way as the HZSM-5 commercial, according to mechanisms shown in literature. The catalytic bed temperature of 600 °C influenced the aromatics yield, indicating that the temperature is an important parameter in the deoxygenation reaction of the pyrolysis products. Finally, the results reinforce circular economics, since it uses industrial waste for catalyst production and an agricultural waste which is converted into high added chemical products.

Acknowledgements

The authors gratefully acknowledge CNPq, CAPES, PETROBRAS (Project – Catalisadores estruturados) and LABTAM/NUPPRAR/UFRN for use of facilities.

References

Al Arni, S., Bosio, B., Arato, E., 2010. Syngas from sugarcane pyrolysis: An experimental study for fuel cell applications. Renew. Energy 35, 29–35.
Ali, M., 2003. Synthesis, characterization and catalytic activity of ZSM-5 zeolites having variable silicon-to-aluminum ratios. Appl. Catal. A 252, 149–162.
Braga, R.M., Melo, D.M.A., Aquino, F.M., Freitas, J.C.O., Melo, M.A.F., Barros, J.M.F., Fontes, M.S.B., 2014. Characterization and comparative study of pyrolysis kinetics of the rice husk and the elephant grass. J. Therm. Anal. Calorim. 115, 1915–1920.
Braga, R.M., Queiroga, T.S., Calixto, G.Q., Almeida, H.N., Melo, D.M.A., Melo, M.A.F., Freitas, J.C.O., Curbelo, F.D.S., 2015. The energetic characterization of pineapple crown leaves. Environ. Sci. Pollut. Res. 22, 18987–18993.
Carlson, T.R., Tompsett, G.A., Conner, W.C., Huber, G.W., 2009. Aromatic production from catalytic fast pyrolysis of biomass-derived feedstocks. Top. Catal. 52, 241–252.
Carrier, M., Loppinet-Serani, A., Denux, D., Lasnier, J.-M., Ham-Pichavant, F., Cansell, F., Aymonier, C., 2011. Thermogravimetric analysis as a new method to determine the lignocellulosic composition of biomass. Biomass Bioenergy 35, 298–307.
Cheng, Y., Huber, G., 2011. Chemistry of furan conversion into aromatics and olefins over HZSM-5: a model biomass conversion reaction. ACS Catal. 1 (6), 611–628.
Cui, M., Zang, S., Lin, W., Meng, C., 2018. Mechanistic study on the synthesis of ZSM-5 from a layered silicate magadiite. Microporous and Mesoporous Materials 265, 63–69.
Demirbaş, A., 1997. Calculation of higher heating values of biomass fuels. Fuel 76, 431–434.
Demirbaş, A., 2000. Mechanisms of liquefaction and pyrolysis reactions of biomass. Energy Convers. Manage. 41, 633–646.
Efika, C.E., Onwudili, J.A., Williams, P.T., 2018. Influence of heating rates on the products of high-temperature pyrolysis of waste wood pellets and biomass model compounds. Waste Manage. 76, 497–506.
Engtrakul, C., Mukarakate, C., Starace, A.K., Magrini, K.A., Rogers, A.K., Yung, M.M., 2016. Effect of ZSM-5 acidity on aromatic product selectivity during upgrading of pine pyrolysis vapors. Catal. Today 269, 175–181.
French, R., Czernik, S., 2010. Catalytic pyrolysis of biomass for biofuels production. Fuel Process. Technol. 91, 25–32.
Gutiérrez-Antonio, C., Gómez-Castro, F.I., de Lira-Flores, J.A., Hernández, S., 2017. A review on the production processes of renewable jet fuel. Renew. Sustain. Energy Rev. 79, 709–729.
Holmes, S.M., Khoo, S.H., Kovo, A.S., 2011. The direct conversion of impure natural kaolin into pure zeolite catalysts. Green Chemistry 13, 1152–1154.
Jia, L.Y., Raad, M., Hamieh, S., Toufaily, J., Hamieh, T., Bettahar, M.M., Mauviel, G., Tarrighi, M., Pinard, L., Dufour, A., 2017. Catalytic fast pyrolysis of biomass: superior selectivity of hierarchical zeolites to aromatics. Green Chem. 19, 5442.
Karmee, S.K., 2018. A spent coffee grounds based biorefinery for the production of biofuels, biopolymers, antioxidants and biocomposites. Waste Manage. 72, 240–254.
Kim, J., Lee, J., Park, J., Kim, J., An, D., Song, I., Choi, J., 2015. Catalytic pyrolysis of lignin over HZSM-5 catalysts: Effect of various parameters on the production of aromatic hydrocarbon. J. Anal. Appl. Pyrol. 114, 273–280.
Kubička, D., Kikhtyanin, O., 2015. Opportunities for zeolites in biomass upgrading—Lessons from the refining and petrochemical industry. Catal. Today 243, 10–22.
Kurnia, I., Karnjanakom, S., Bayu, A., Yoshida, A., Rizkiana, J., Prakoso, T., Abudula, A., Guan, G., 2017. In-situ catalytic upgrading of bio-oil derived from fast pyrolysis of lignin over high aluminum zeolites. Fuel Process. Technol. 167, 730–737.
Lorenzetti, C., Conti, R., Fabbri, D., Yanik, J., 2016. A comparative study on the catalytic effect of H-ZSM5 on upgrading of pyrolysis vapors derived from lignocellulosic and proteinaceous biomass. Fuel 166, 446–452.
Maneffa, A., Priecel, P., Lopez-Sanchez, J.A., 2016. Biomass-derived renewable aromatics: selective routes and outlook for p-Xylene commercialisation. ChemSusChem 9, 2736–2748.
Mei, Q., Shen, X., Liu, H., Han, B., 2018. Selectively transform lignin into value-added chemicals. Chin. Chem. Lett.
Mihalcik, D.J., Mullen, C.A., Boateng, A.A., 2011. Screening acidic zeolites for catalytic fast pyrolysis of biomass and its components. J. Anal. Appl. Pyrol. 92, 224–232.
Mohan, D., Pittman, C.U., Steele, P.H., 2006. Pyrolysis of wood/biomass for bio-oil: a critical review. Energy Fuels 20, 848–889.
Mullen, C.A., Boateng, A.A., 2010. Catalytic pyrolysis-GC/MS of lignin from several sources. Fuel Process. Technol. 91, 1446–1458.
Narayanan, S., Vijaya, J.J., Sivasanker, S., Ragupathi, C., Sankaranarayanan, T.M., Kennedy, L.J., 2016. Hierarchical ZSM-5 catalytic performance evaluated in the selective oxidation of styrene to benzaldehyde using TBHP. J. Porous Mater. 23, 741–752.
Onwudili, J.A., Muhammad, C., Williams, P.T., 2018. Influence of catalyst bed temperature and properties of zeolite catalysts on pyrolysis-catalysis of a simulated mixed plastics sample for the production of upgraded fuels and chemicals. J. Energy Inst. https://doi.org/10.1016/j.joei.2018.10.001 (in press).

Raviv, O., Broitman, D., Ayalon, O., Kan, I., 2018. A regional optimization model for waste-to-energy generation using agricultural vegetative residuals. Waste Manage. 73, 546–555.
Reshamwala, S., Shawky, B.T., Dale, B.E., 1995. Ethanol production from enzymatic hydrolysates of AFEX-treated coastal bermudagrass and switchgrass. Appl. Biochem. Biotechnol. 51, 43.
Sabarish, R., Unnikrishnan, G., 2017. Synthesis, characterization and catalytic activity of hierarchical ZSM-5 templated by carboxymethyl cellulose. Powder Technol. 320, 412–419.
Santana, J.A., Carvalho, W.S., Ataíde, C.H., 2018. Catalytic effect of ZSM-5 zeolite and HY-340 niobic acid on the pyrolysis of industrial kraft lignins. Ind. Crops Prod. 111, 126–132.
Shah, S.A.Y., Zeeshan, M., Farooq, M.Z., Naveed, A., Naseem, I., 2019. Co-pyrolysis of cotton stalk and waste tire with a focus on liquid yield quantity and quality. Renew. Energy 130, 238–244.
Stefanidis, S.D., Kalogiannis, K.G., Iliopoulou, E.F., Lappas, A.A., Pilavachi, P.A., 2011. In-situ upgrading of biomass pyrolysis vapors: catalyst screening on a fixed bed reactor. Bioresour. Technol. 102, 8261–8267.
Wang, K., Zhang, J., Shanks, B.H., Brown, R.C., 2015. Catalytic conversion of carbohydrate-derived oxygenates over HZSM-5 in a tandem micro-reactor system. Green Chem. 17, 557.
Wang, K., Kim, K.H., Brown, R.C., 2014. Catalytic pyrolysis of individual components of lignocellulosic biomass. Green Chem. 16, 727–735.
Wu, S., Shen, D., Hu, J., Zhang, H., Xiao, R., 2016. Role of β-O-4 glycosidic bond on thermal degradation of cellulose. J. Anal. Appl. Pyrol. 119, 147–156.
Xue, T., Wang, Y.M., He, M.-Y., 2012. Facile synthesis of nano-sized NH_4-ZSM-5 zeolites. Microporous Mesoporous Mater. 156, 29–35.
Yang, H., Yan, R., Chen, H., Lee, D.H., Zheng, C., 2007. Characteristics of hemicellulose, cellulose and lignin pyrolysis. Fuel 86, 1781–1788.
Yang, Y., Lv, G., Deng, L., Lu, B., Li, J., Zhang, J., Shi, J., Du, S., 2017. Renewable aromatic production through hydrodeoxygenation of model bio-oil over mesoporous Ni/SBA-15 and Co/SBA-15. Microporous Mesoporous Mater. 250, 47–54.
Yu, Y., Li, X., Su, L., Zhang, Y., Wang, Y., Zhang, H., 2012. The role of shape selectivity in catalytic fast pyrolysis of lignin with zeolite catalysts. Appl. Catal. A 447–448, 115–123.
Yue, Y., Liu, H., Yuan, P., Li, T., Yu, C., Bi, H., Bao, X., 2014. From natural aluminosilicate minerals to hierarchical ZSM-5 zeolites: A nanoscale depolymerization–reorganization approach. Journal of Catalysis 319, 200–210.
Yue, Y., Liu, H., Yuan, P., Yu, C., Bao, X., 2015. One-pot synthesis of hierarchical FeZSM-5 zeolites from natural aluminosilicates for selective catalytic reduction of NO by NH_3. Sci. Rep. 5, 9270.
Zhang, C., Chen, H., Zhang, X., Wang, Q., 2017. TPABr-grafted MWCNT as bifunctional template to synthesize hierarchical ZSM-5 zeolite. Mater. Lett. 197, 111–114.